ELSEVIER

International Journal of Mass Spectrometry 207 (2001) 73–96

International Journal of Mass Spectrometry

Mechanisms of energy deposition in infrared matrix-assisted laser desorption/ionization mass spectrometry

Christoph Menzel, Klaus Dreisewerd, Stefan Berkenkamp and Franz Hillenkamp*

Institut für Medizinische Physik und Biophysik, Universität Münster, D-48149 Münster, Germany

Received 19 September 2000; accepted 18 December 2000

Abstract

The mechanisms of energy deposition in matrix-assisted laser desorption/ionization mass spectrometry with infrared lasers (IR-MALDI-MS) have been evaluated in a series of experiments. In a first part, the threshold fluences for the generation of IR-MALDI spectra were determined between 2.7 and 4.0 μm wavelength with an optical parametric oscillator as a tunable laser source for nine solid state and two liquid matrices of different chemical structure and compared to the infrared absorption spectra of the compounds. Preliminary spectra of IR-MALDI in the wavelength range of 1.45–1.75 μm are also presented using the overtone vibrations of a glycerol matrix. Matrices were chosen with regard to their IR-MALDI performance and to allow conclusions on the IR-absorption mechanisms. Whereas the wavelength dependence of the threshold fluence for non–hydrogen-bound C–H vibrations essentially follows the absorption spectrum of this functional group, strong discrepancies between the spectral dependence of threshold fluences and IR-absorption spectra were found for the vibrations of O–H and N–H groups around 3-μm wavelength that form strong intermolecular and intramolecular hydrogen bonds. In a second part, experiments are described that interrogate the two most probable mechanisms for the observed deviation of the threshold fluence behavior from the wavelength course of the IR-absorption spectra, that is, absorption by either free or weakened O–H and N–H stretching modes or by residual free water. All investigations were performed with glycerol and succinic acid as examples for common liquid and solid state matrices for IR-MALDI. For glycerol, a fluence-dependent, dynamic change in absorption during the laser pulse was revealed by laser transmission measurements on thin glycerol layers. This effect, characterized by a significant blue shift of the O–H stretch absorption, can be attributed to a weakening of intermolecular hydrogen bonds caused by the transient laser heating of the sample. Taking this effect into account, a good correspondence of the wavelength dependence of the threshold fluence with the infrared absorption under IR-MALDI conditions is derived for glycerol. For succinic acid, in contrast, the identification of the predominant absorption mechanism in the 3-μm wavelength range appears more difficult. A fluence-dependent absorption was not detected in laser transmission experiments with succinic acid single crystals. A change in analyte-to-matrix ratio, with the intention of inducing free absorbers near crystal defects, also did not influence the wavelength dependence of the threshold fluences. However, an influence of the surface-to-volume ratio on the wavelength-dependent threshold fluences was found by a comparison of three different preparation techniques for succinic acid, indicating a putative influence of weakly hydrogen-bound surface absorbers. In combination with the detailed analysis of the wavelength dependence of the threshold fluence given from the first part, a determination of the IR-MALDI process for succinic acid based on the absorption by weakly hydrogen-bound hydroxyl groups is suggested. No evidence for a significant contribution of residual free water absorption to the low-threshold fluences around 3-μm wavelength was found by monitoring a possible change in threshold fluence at the phase transition from water to ice and by reducing the analyte hydration and varying the water content in glycerol preparations. Also, in preparations with frozen hydrated proteins without organic matrices, the

* Corresponding author. E-mail hillenk@uni-muenster.de

1387-3806/01/$20.00 © 2001 Elsevier Science B.V. All rights reserved
PII S1387-3806(01)00363-3

wavelength dependence of the threshold fluence did not reflect the spectral absorption of ice, supporting the assumption of a rather minor role of the absorption by residual water in IR-MALDI. (Int J Mass Spectrom 207 (2001) 73–96) © 2001 Elsevier Science B.V.

Keywords: IR-MALDI; Optical parametric oscillator; Threshold fluence; Wavelength dependence; Absorption model

1. Introduction

Since its invention, ultraviolet (UV) lasers have been employed almost exclusively in matrix-assisted laser desorption/ionization mass spectrometry (MALDI-MS) [1], although the relatively soft conditions of IR desorption/ionization were reported to be of advantage in the analysis of fragile samples including large nucleic acids [2–7]. A variety of different IR laser sources are commercially available nowadays. Whereas fixed-frequency lasers like erbium solid state lasers emitting at wavelengths near 3 μm [2,8] or TEA-CO_2 gas lasers emitting at wavelengths of $\sim$10 μm [4,9] have been used for almost a decade in IR-MALDI-MS, more recent studies employed optical parametric oscillators (OPO) [3,10–15] or a free electron laser (FEL) [16–19] as wavelength tunable IR-laser sources.

The minimum necessary laser fluence for the detection of MALDI ions (threshold fluence) and its dependence on various parameters like laser pulse width, size of irradiated area, or laser wavelength are commonly viewed as key parameters for a better understanding of the desorption/ionization processes. Linear absorption assumed, the (threshold) fluence multiplied by the wavelength dependent absorption coefficient equals the energy deposited per unit volume of the sample, which in turn, can be directly compared to material parameters such as the heat of fusion and the enthalpy of sublimation. A good correlation of the threshold fluence with the reciprocal of the matrix absorbance has indeed been found in UV-LDI/MALDI [20–24]. Hence a matrix-specific, constant energy per unit volume is deposited at threshold, independent of the wavelength. For IR-MALDI, a more complicated dependence of the threshold fluence on the matrix absorption has been reported in several studies. The interpretation and comparison of the different results is difficult because different laser systems and sample preparation techniques have been employed, and only a few matrices have been investigated so far. Using the Vanderbilt FEL laser, Cramer et al. found a minimal threshold fluence around a wavelength of 2.94 μm, although the peak absorption of succinic acid and fumaric acid is located at 3.3–3.4 μm and even at 4.1 μm for nicotinic acid [17]. For the C=O stretch vibration around 6 μm, however, a good correspondence was observed in this study between threshold fluences minima and absorption maxima for these matrices. In two other FEL studies by Hess et al. and Papantonakis et al., however, a small blue shift for the C=O band has been reported for succinic acid [18,19]. In a study with a Cr:LiSAF laser pumped KTA-OPO laser, Sadeghi et al. did not find a qualitative correlation between the IR-MALDI performance and the matrix absorbance for a urea and a succinic acid matrix in the investigated narrow wavelength range of 2.88–2.96 μm [11]. Similar results were obtained by Caldwell et al. and Sheffer et al. in the wavelength range of the O–H, N–H, and C–H stretch vibrations using a Nd:YAG pumped KTP-OPO laser and a special preparation on a nitrocellulose layer [10,13]. A good qualitative correlation between threshold fluence and the reciprocal matrix absorption was found in the study of Sheffer et al. for a four-nitroanilin matrix and its C–H and N–H stretch vibrations, whereas succinic and caffeic acid with strong O–H absorption bands showed a blue shift of the threshold in agreement with the FEL studies [13]. A comparable behavior for caffeic acid was reported by Durrant et al. [15].

In these studies, the most pronounced discrepancies between spectral absorption and the wavelength-dependent threshold fluence or the IR-MALDI performance were systematically observed around 3 μm wavelength, which covers the spectral range of free

(non–hydrogen-bound) O–H and N–H stretch vibrations and the broad and strong absorption of the water O–H vibrations near 2.9 μm wavelength. To explain the discrepancies, a substantial absorption of free or weakly hydrogen-bound O–H or N–H groups (free absorber model) as well as an additional absorption by residual water (residual water model) have, therefore, been proposed [10,12,13,15,17–19,25]. However, no direct experimental proof for either of these models has been presented to date.

To address these questions, a series of experiments has been performed. Their results are reported in the two parts of this publication. In the first part, a comprehensive investigation of the influence of the laser excitation wavelength between 1.45 and 4.0 μm on the threshold fluence and the IR-MALDI performance for various matrices is presented. These include succinic, caffeic, and nicotinic acid, which have also been examined in former studies by other authors. Correspondences and contradictions of the observed parametric dependence to the free absorber and/or to the residual water model are discussed. On the basis of these results, different experiments have been performed to evaluate both models for the energy deposition. These results are presented in the second part of this publication.

2. Part I: Wavelength-dependent threshold fluences for matrices of different chemical structure

2.1. Experimental

2.1.1. Mass spectrometer

All experiments were carried out with an in-house-built single-stage reflectron time-of-flight (REF-TOF) mass spectrometer of 3.5 m equivalent flight length. For the determination of threshold fluences, the mass spectrometer was used in the linear TOF mode (LIN-TOF) with a flight length of 2.1 m. For the evaluation of the mass spectrometric performance, the REF-TOF mode was used because of a better mass resolution and the possibility to estimate the extent of metastable decay from the REF-TOF mass spectra. All experiments reported here were carried out in the positive ion mode. Ions were accelerated through a total potential difference of 16–27.5 kV in a split extraction source under static extraction conditions. A relatively weak electric field strength of 200–400 V/mm in the first extraction region was found favorable for IR-MALDI and was used throughout all experiments. Venetian-blind secondary electron multipliers (SEM; 9643/A, Emi-Thorn, Ruislip, UK) equipped with a conversion dynode mounted 10 mm in front of the first dynode of the SEM were used for ion detection. For analytes $>$10 kDa, like cytochrome C, the potential between the conversion dynode and the SEM was set to 15 kV to increase the ion signal by efficient detection of secondary ions, produced at the conversion dynode. Signals were processed by a transient recorder (LeCroy 9350A, Chestnut Ridge, NY), and the digitized data were transferred to a PC for storage and further evaluation. Samples were observed in situ with a CCD camera at a resolution of $\sim$20 μm.

2.1.2. Laser and laser optics

A wavelength-tunable OPO laser system (Mirage 3000B, Continuum, Santa Clara, CA) pumped by the fundamental and second harmonic of a Nd:YAG laser (Surelite II-10, Continuum) was used for IR-MALDI, comparable to the two OPO systems employed in former studies [3,10,13,14,26]. The system generates a 1.45–2.12-μm signal and a 2.12–4.0-μm idler wave in a two-stage nonlinear parametric process. Wavelength tuning is achieved by computer-controlled angle phase matching of the potassium titanyl phosphate (KTP) nonlinear crystals.

Signal and idler waves of the final stage were found to be not perfectly collinear in the output beam and could, therefore, be separated by a small aperture. Residual photons in the output beam with wavelengths $<$1.9 μm were completely blocked by a germanium substrate at Brewster's angle. For experiments in the midinfrared region from 1.45 to 2.12 μm, the Ge substrate was removed, and the Nd:YAG fundamental pump beam for the second OPO stage was blocked to prevent generation of 3-μm photons via parametric amplification. Single laser pulses of 6

ns in width were selected by the Q-switch of the Nd:YAG pump laser. For wavelengths <3.1 μm, the shot-to-shot pulse energy stability was determined to about $\pm 2\%$, while variations up to $\pm 5\%$ were observed for longer wavelengths. Silver-coated mirrors were used for beam steering. The OPO laser beam was focused onto the target by an uncoated CaF_2 lens of 110 mm focal length (at 3-μm wavelength) and coupled into the mass spectrometer through an uncoated CaF_2 vacuum window.

For wavelengths between 2.75 and 3.05 μm, the desorption energy was adjusted by angle variation of dielectric-coated CaF_2 substrates (Laser Optik GmbH, Garbsen, Germany) with a computer-controlled stepper-motor unit. For all other wavelengths between 2.0 and 4.0 μm, the energy was adjusted by angle variation of uncoated germanium substrates. Although germanium exhibits a high index of refraction of about four in the investigated spectral range, the dynamic range in attenuation from normal incidence to Brewster's angle was relatively small compared to the attenuation by the dielectric-coated CaF_2 substrates. Several Ge substrates were therefore combined in a counter-rotating set-up to compensate for beam displacement during variation of the angle. For the experiments with wavelengths <2.0 μm, only a rough energy adjustment with stacks of metal grids of different geometrical transmission was applied.

2.1.3. Fluence and wavelength measurements

The relevant parameters, laser pulse energy, irradiated area, and laser wavelength, were carefully monitored throughout all experiments. The laser pulse energies were measured off-line with a high-precision commercial energy meter (Laser Precision, Yorkville, NY) by placing the energy meter directly into the beamline, immediately after the mass spectrometric threshold determinations. Laser pulse energies were averaged over 25 consecutive single laser pulses. Fluences were calculated by dividing the measured laser pulse energies by the irradiated area, determined as described below. Transmission losses caused by all optical elements were determined separately and taken into account. The threshold fluence was defined in this study as the lowest laser fluence for which $>10\%$ of the spectra exhibited an analyte signal-to-noise ratio of at least 3 : 1, equivalent to the definition used in a previous FEL study [17]. For the determination of the threshold fluence, typically five single-threshold measurements with separate samples were carried out per wavelength. From this set of data, a mean threshold fluence and standard deviation was calculated. The fluence error, resulting from a variation of the size of the irradiated area as a function of wavelength, was found to be the most critical issue in the experiments. The problem is even aggravated, as a strong dependence of the threshold fluence on the size of the irradiated area has been found recently for IR-MALDI [27]. An irradiation with a homogeneous top-hat beam profile by imaging the exit face of an optical fiber onto the sample, as described for an Er:YAG laser [27], would have been most desirable for these experiments. Unfortunately, not enough energy could be transmitted through the sapphire fiber in the full wavelength range investigated. All experiments reported here were, therefore, performed with the near-Gaussian far-field TEM_{00} beam profile of the OPO laser.

The size of the irradiated area was determined by burn patterns on black photographic paper (Agfa-Gevaert AG, Leverkusen, Germany), mounted on the target. To calibrate the burn patterns, laser beam profiles in the focal plane were measured in a separate experiment by scanning the beam cross section with a pinhole (20 μm diameter) and recording of the transmitted energy with a high-precision energy meter. For fluences $>10^4$ Jm^{-2}, the diameter of the burn patterns was found to nearly equal to that at the $1/e^2$ intensity value, as determined by the pinhole method, independent of the wavelength. The laser spot size on the sample was maintained constant over the full wavelength range by varying the distance between the focusing lens and the sample, according to the Sellmeier dispersion relation for CaF_2 [28]. The irradiated area was elliptical because of the angle of 45° between target normal and the IR laser beam, with a size of $(16.3 \pm 1.7) \times 10^{-9}$ m^2.

The wavelengths of the OPO output beams were checked with a monochromator (M4 QII, Carl Zeiss GmbH, Oberkochen, Germany) up to a wavelength of

2.4 μm and, for longer wavelengths, by narrow-band filters (Infrared Engineering, Maldon, Essex, England) at 2.4, 3.0, and 3.4 μm. A wavelength offset of 45 nm relative to the calibration of the manufacturer was observed and corrected for in all experiments. The bandwidth of the OPO laser is specified by the manufacturer to ~10 nm at a wavelength of 3 μm.

2.1.4. Infrared spectroscopy

Standard transmission spectra were taken from a variety of databases [29–31]. These alkali halide pellet (KBr/KI) or nujol mull (for solid samples) and thin film (for liquids) transmission spectra are intended for compound identification and do not provide absolute values for the absorption coefficients. However, at least for FT-IR spectra, the accuracy of the qualitative spectral dependence is high, in particular around the peak absorption wavelength [30]. All spectral data in this publication are given for wavelength as well as wavenumber to make the comparison with published data easier. In case of the nujol mull, the comparison to the measured spectral threshold behavior is disturbed by the overlapping C–H bands of the paraffin oil around 3.4 μm in the IR-transmission spectra. Therefore, nujol mull bands are displayed shaded in the transmission spectra of the figures for a better differentiation of matrix and paraffin absorption. Except for the spectral region of nujol absorption, spectra recorded with the alkali–halide or nujol mull technique agree well with each other. A good correspondence of these spectra to the FT-IR absorption spectra of typical IR-MALDI preparations on an IR-transparent plate was, moreover, demonstrated in two former studies [17,25]. This indicates a good, qualitative representation of the wavelength-dependent absorption in the crystalline environment by the spectra in the literature.

2.1.5. Sample preparation

Succinic acid, adipic acid, malic acid, DL-quinic acid, thiourea, and L-tryptophane were dissolved in H_2O to concentrations of 20–30 g/L. Phloroglucinol and caffeic acid were dissolved to a concentration of 20 g/L in a 1 : 1 mixture of water and ethanol. Unless specifically noted, solid matrix samples were prepared by the standard dried-droplet method, mixing 1 μL of a 10^{-4} M aqueous solution of cytochrome C (horse heart) with 2 μL of the matrix solution, followed by drying in a stream of cold air. Liquid matrix samples of glycerol and triethanolamine were prepared on-target by thoroughly mixing the neat matrix liquids with the aqueous analyte solution in a 1 : 1 volume ratio. Before insertion of the samples into the high vacuum of the sample chamber, most of the water solvent was gassed off at a pressure of $\sim 10^{-2}$ mbar in the transfer lock of the mass spectrometer. All chemicals were purchased from Sigma (Deisenhoven, Germany) or Fluka Chemica (Buchs, Switzerland) and used without further purification, as is also true for the determination of the transmission spectra.

2.2. Results and discussion

2.2.1. Dependence of the MALDI performance and the threshold fluence on the laser wavelength

In the following, the wavelength dependence of threshold fluence and MALDI performance are presented for various matrices along with the IR-transmission spectra of the compounds ordered by their chemical structure.

2.2.2. Dicarboxylic acids

Fig. 1a–c shows the dependence of the threshold fluence on the laser wavelength for three dicarboxylic acids. Adipic acid (Fig. 1b) and malic acid (Fig. 1c) were chosen as test compounds because they differ from the standard IR matrix succinic acid (Fig. 1a) only in an additional CH_2 and O–H group, respectively. Although the transmission spectra of the three matrices (Fig. 1d–f) exhibit significant differences, particularly if succinic and adipic acid are compared with malic acid, the wavelength dependencies of the threshold fluence (Fig. 1a–c) are surprisingly similar. For succinic acid and adipic acid, the threshold begins to decrease strongly at ~2.80 μm and reaches a plateau of nearly constant low-threshold fluences at ~2.90 μm without a corresponding absorption band in the transmission spectra below ~3.20 μm. For malic acid (Fig. 1c), the minimum threshold fluence is already reached at a wavelength of 2.80 μm, still

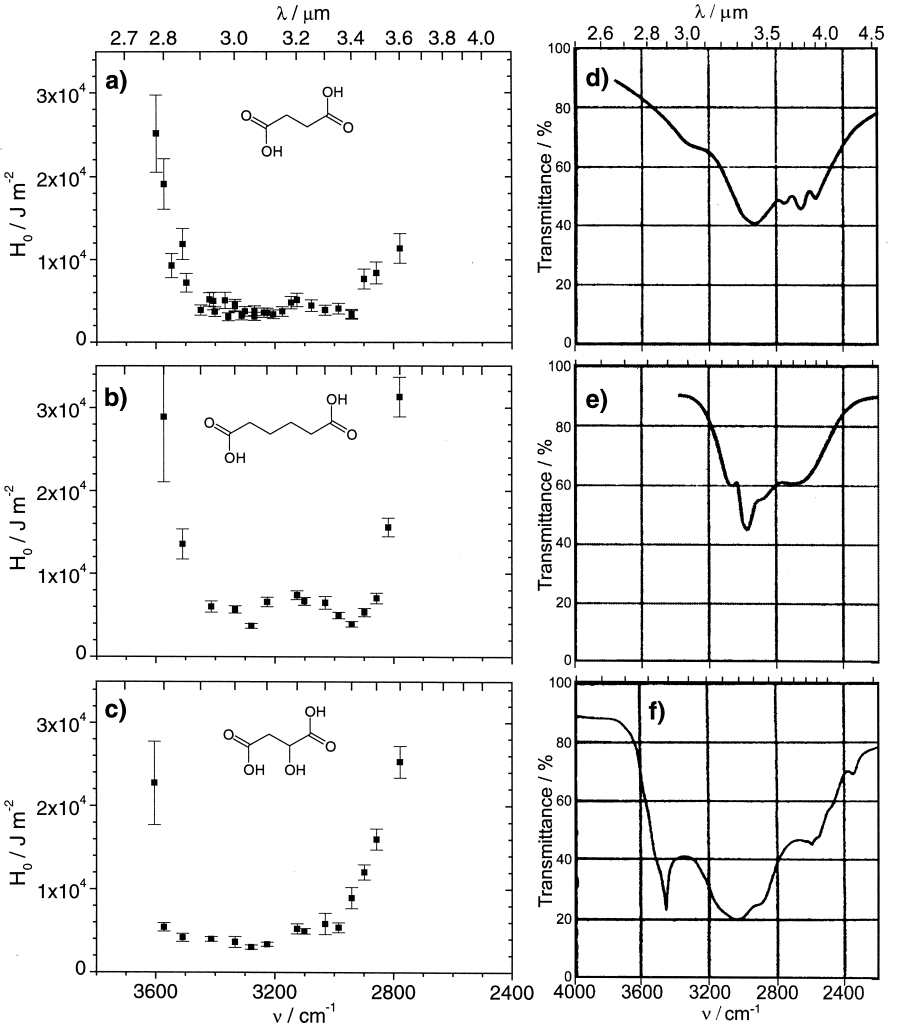

Fig. 1. Threshold fluence $H_0(\lambda)$ for desorption of cytochrome C ions from different dicarboxylic acids and IR transmittance as a function of wavenumber ν and wavelength λ respectively: (a) $H_0(\lambda)$ for succinic acid; (b) $H_0(\lambda)$ for adipic acid; (c) $H_0(\lambda)$ for malic acid. IR-transmission spectra of (d) succinic acid, (e) adipic acid, (f) malic acid. The IR-transmission spectra were recorded with the alkali halide method. (d–f) adapted from [29] with permission.

substantially below the additional absorption band of the noncarboxylic O–H vibration of this matrix (Fig. 1f).

For all three matrices the plateau of low-threshold fluences ends around the peak absorption of the carboxylic O–H vibration in the 3.3–3.5 μm region. This strong and broad peak absorption band is caused by the formation of strong hydrogen bonds for the head-to-head dimerized carboxyls in the crystalline solid state and is red shifted by several hundred nanometers compared with the free O–H stretch vibration between 2.81 and 2.86 μm [32]. For longer wavelengths, the absorption of all three matrices decreases again, although disturbed to some extent by the less intense C–H absorption [32]. For these wavelengths, a good qualitative correspondence of inverse absorption and threshold fluence is found.

The mass spectrometric performance strictly follows the wavelength dependence of the threshold

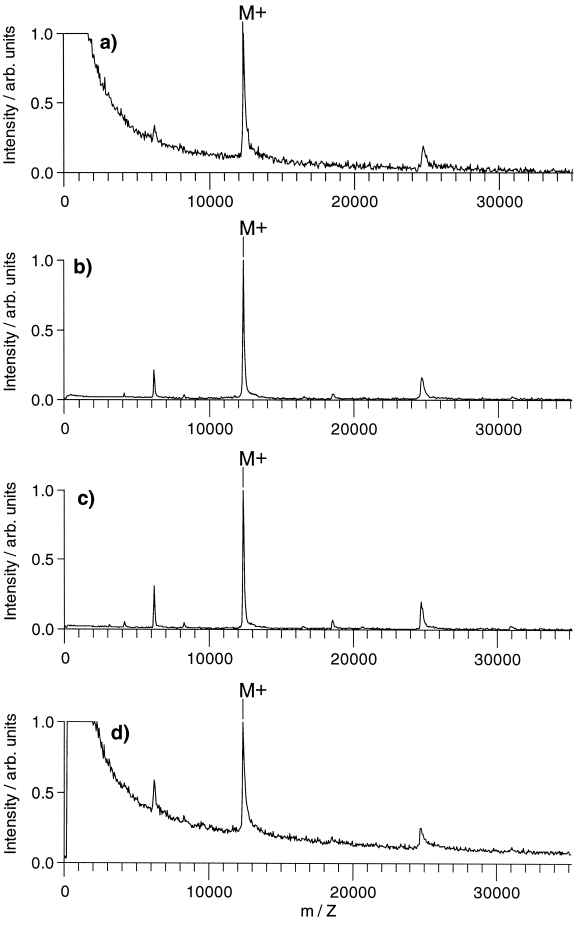

Fig. 2. REF-TOF IR-MALDI mass spectra of cytochrome C desorbed from a succinic acid matrix at different wavelengths λ: (a) λ=2.79 μm; (b) λ=2.94 μm; (c) λ=3.40 μm; (d) λ=3.60 μm. Each spectrum represents the sum of 15 single-shot mass spectra.

fluence: The lower the threshold, the better the spectra quality in terms of signal-to-noise ratio and low mass background. This is exemplarily shown for succinic acid in Fig. 2. Spectra taken with wavelengths >3.50 or <2.85 μm (for malic acid <2.80 μm) suffer from a strong matrix background (Fig. 2a,d). Interestingly, even at the elevated laser fluences needed for low-absorption wavelengths, only a very limited metastable fragmentation of cytochrome was observed, as documented by a steep rising slope of the ion signals in the reflectron mode.

In contrast to prior studies by Cramer et al. and Sheffer et al. [13,17], relatively low threshold fluences and a good mass spectrometric performance was found in our investigations for the succinic acid matrix in the wavelength range of 3.3–3.4 μm.

2.2.3. Monocarboxylic acids

The wavelength dependence of the threshold fluence for three monocarboxylic acids, nicotinic acid, caffeic acid, and quinic acid, is shown along with the corresponding nujol mull transmission spectra in Fig. 3. The wavelength dependence of the threshold fluences of these matrices is similar to that of the dicarboxylic acids in Fig. 1, with the exception of nicotinic acid in the range of 3.6–4.0 μm. The low threshold fluence for nicotinic acid at these wavelengths (Fig. 3a) tracks reasonably well with its absorption (Fig. 3d), whereas the correspondence between the transmission spectrum of nicotinic acid and the threshold behavior is poor for shorter wavelengths.

Caffeic acid and quinic acid have strong absorption bands (Fig. 3e,f) and low threshold fluences (Fig. 3b,c) around 2.9 μm, but for both matrices, a decrease in threshold fluence is already observed for wavelengths as low as 2.75 μm, substantially lower than the O–H absorption band. The strong modulations in the transmission spectrum around 3 μm (Fig. 3e,f) are also not reflected in the spectral threshold dependence for these two matrices. The minimum in the threshold fluence at 3.3 μm for caffeic acid and at 3.5 μm for quinic acid are close to the peak absorption of the stretching vibration of associated carboxylic O–H groups in both matrices. Note that the corresponding bands in the transmission spectra are disturbed by nujol background absorption bands (Fig. 3e,f).

Of all tested matrices, caffeic acid exhibited the best MALDI-MS performance for wavelengths <2.8 μm. Nicotinic acid, in contrast, showed the best performance for wavelengths >3.7 μm, in accordance with the relatively low threshold of nicotinic acid in this wavelength range.

In the FEL study by Cramer et al., the threshold fluences for desorption of insulin ions from a nicotinic acid matrix were found to monotonically increase from 3.0 μm to ~4 μm in contradiction to the results

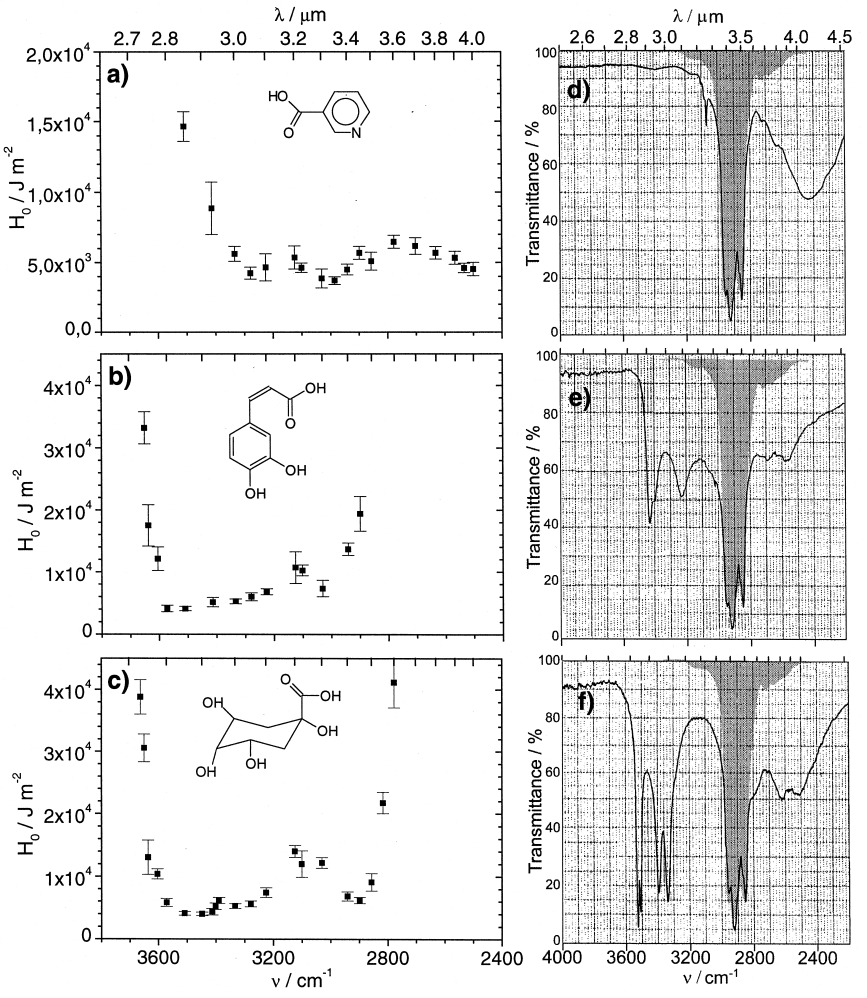

Fig. 3. Threshold fluence $H_0(\lambda)$ for desorption of cytochrome C ions from different monocarboxylic acids and IR transmittance as a function of wavenumber ν and wavelength λ, respectively: (a) $H_0(\lambda)$ for nicotinic acid; (b) $H_0(\lambda)$ for caffeic acid; (c) $H_0(\lambda)$ for quinic acid. IR-transmission spectra of (d) nicotinic acid, (e) caffeic acid, (f) quinic acid. IR-transmission spectra were recorded out of nujol mull. The shaded areas indicate the wavelength range of nujol mull background absorption. (d–f) adapted from [30] with permission.

in Fig. 3a [17]. For caffeic acid, a similarly good IR-MALDI performance was found for wavelengths <2.9 μm by Sheffer et al. and Durrant et al. [13,15]. The threshold characteristic in the study by Sheffer et al. for caffeic acid, however, showed a minimum in fluence at ~ 2.9 μm, substantially higher than in our study [13]. Sheffer et al. also reported some difficulties in obtaining spectra for a caffeic acid matrix and wavelengths >3.05 μm in disagreement with our findings.

2.2.4. Urea and amino acids

Figure 4 shows the threshold fluence as a function of wavelength and the IR transmission spectra for thiourea and L-tryptophane. Different N–H stretch vibration modes determine the IR-absorption characteristic for these molecules in the wavelength range from 2.9 to 3.5 μm (Fig. 4c,d). For thiourea, the course of the threshold fluence (Fig. 4a) tracks the envelope of the transmission spectrum (Fig. 4c) quite well. However, a small blue shift in the threshold

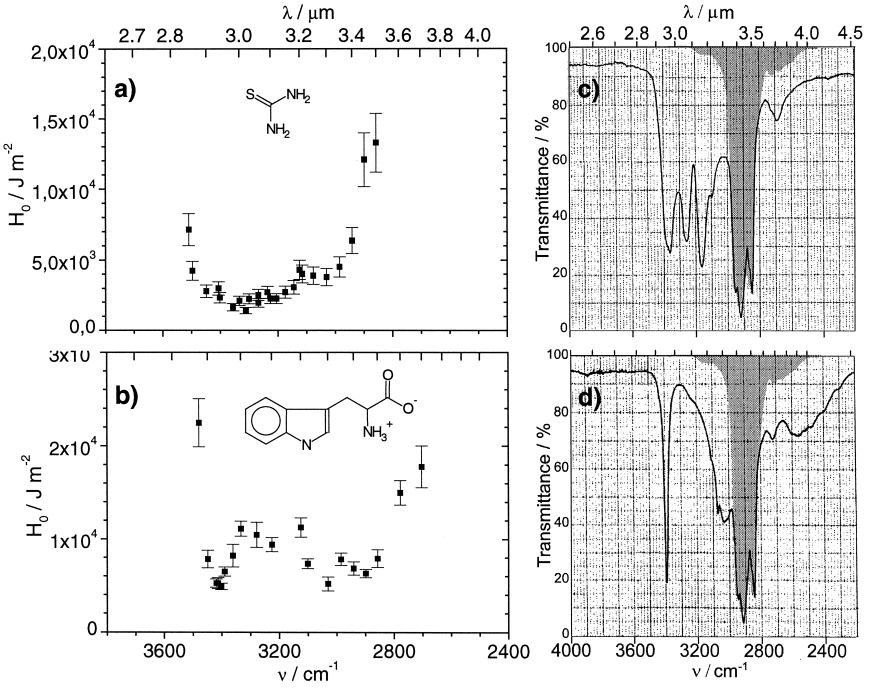

Fig. 4. Threshold fluence $H_0(\lambda)$ for desorption of cytochrome C ions from urea and the amino acid tryptophane and IR transmittance as a function of wavenumber ν and wavelength λ, respectively: (a) $H_0(\lambda)$ for thiourea; (b) $H_0(\lambda)$ for tryptophane. IR-transmission spectra of (c) thiourea, (d) tryptophane. IR-transmission spectra were recorded out of nujol mull. The shaded areas indicate the wavelength range of nujol mull background absorption. (c–d) adapted from [30] with permission.

dependence is evident for wavelengths near 2.9 μm. The distinct bands, typically found for asymmetric and symmetric vibrations of the N–H group, were not observed in the threshold dependence. The sharp indole band in the tryptophane transmission spectrum at 2.94 μm (Fig. 4d) can, however, be recognized in the threshold-wavelength dependence (Fig. 4b), albeit broadened. The substantial differences in absorption (a rise in transmission from 20% to 90% corresponds to a ~15-fold decrease in absorbance) in the range between the indole and the broad NH_3^+ band near 3.3 μm are only barely reflected in the threshold fluence spectrum of tryptophane.

Sheffer et al. and Sadeghi et al. investigated the midinfrared wavelength dependence of the IR-MALDI performance for the N–H stretching modes of 4-nitroaniline and urea [11,13]. For 4-nitroaniline, a qualitatively good correspondence of IR absorbance and threshold fluence was found by Sheffer et al., although the threshold fluence at 2.9 μm was lower than expected from the IR transmission spectrum [13]. A wavelength scan over the two pronounced absorption bands of urea around 2.95 μm, performed in the study of Sadeghi et al. [11], did not reveal a significant influence of these modulations on the IR-MALDI spectra, well in agreement with our findings for thiourea.

2.2.5. Phenols and alcohols

Matrices with phenolic and alcoholic hydroxyl groups, solid phloroglucinol as well as the liquid matrices glycerol and triethanolamine, have also been tested (Fig. 5). For phloroglucinol, only a poor correlation between threshold fluence and IR transmittance was found at all wavelengths (Fig. 5a,d). Phloroglucinol was also the only solid matrix in this study that showed a relatively high threshold fluence and strong IR-MALDI spectra degradation (spectra not shown) in the wavelength range of the peak absorption at about 3.13 μm. The low threshold between 2.82 and

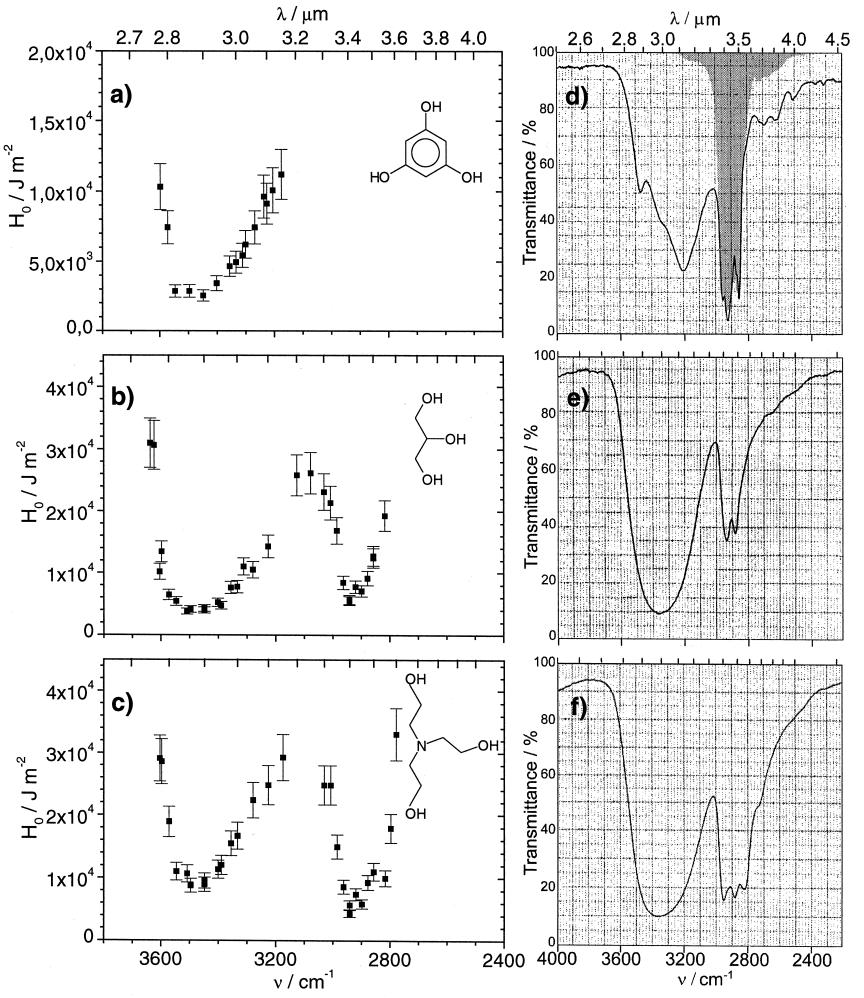

Fig. 5. Threshold fluence $H_0(\lambda)$ for desorption of cytochrome C ions from different alcoholic and phenolic matrices and IR transmittance as a function of wavenumber ν and wavelength λ, respectively: (a) $H_0(\lambda)$ for phloroglucin; (b) $H_0(\lambda)$ for glycerol; (c) $H_0(\lambda)$ for triethanolamine. IR-transmission spectra of (d) phloroglucin from of a nujol mull (the shaded area indicates the wavelength range of nujol mull background absorption); (e) glycerol; (f) triethanolamine. (d–f) adapted from [30] with permission.

2.90 μm amounts to a ~250-nm blue shift of the O–H absorption band. In contrast, for glycerol (Fig. 5b,e), as well as for triethanolamine (Fig. 5c,f), the qualitative correspondence of transmission spectra and threshold fluence appears rather good at first sight. A closer investigation of the 3.0-μm region, however, reveals that the strong O–H absorption band is also blue shifted by ~130 nm in the wavelength dependence of the threshold fluence for both matrices. In contrast, threshold fluences in the region of the C–H stretching vibrations around 3.4 μm scale very well with the IR transmittance, partly revealing even small modulations in absorbance. It should also be noted that a significantly lower threshold fluence for the O–H absorption around 2.9 μm as compared to that of the C–H stretch absorption near 3.4 μm, as suggested by the transmission spectra, is not found in the threshold fluence dependencies.

As for the solid matrices, best spectra for glycerol and triethanolamine of comparatively high quality were observed for wavelengths with minimal threshold fluences.

The above results for glycerol differ to some extent from those reported previously by Caldwell and Murray [26]. A maximum signal intensity for bradykinin around 2.8 μm wavelength was reported in this study for a glycerol/water/nitrocellulose mixture matrix, whereas no analyte signals were observed for wavelengths >3.1 μm [26].

2.2.6. Overtone region

For succinic acid and glycerol, the IR-MALDI wavelength studies were also extended to the overtone region of O–H, N–H, and C–H stretching vibrations in the range between 1.45 and 2.0 μm. This spectral range is of special interest because of the potential use of laser diodes as IR-MALDI light sources. High-power laser diodes emitting in this wavelength regime are widely used at 1.35 or 1.55 μm wavelength in high-transmission fiber optical telecommunication systems.

Attempts to generate cytochrome C mass spectra from a succinic acid matrix were not successful, in agreement with the study of Caldwell et al. [10]. These authors also investigated the overtone region between 1.45 and 1.7 μm with succinic acid and caffeic acid as matrices but did not obtain any spectra. In our study, IR-MALDI spectra could, however, be acquired if glycerol was used as matrix. The threshold fluence dependence of the fundamental absorption bands of glycerol can be recovered for the second harmonics as well. Spectra of cytochrome C could be obtained around 1.45 (Fig. 6a) and 1.7 μm wavelength but not around 1.6 μm. Compared with optimal spectra obtained with a pure glycerol matrix in the 3-μm wavelength range (Fig. 6b), a poor signal-to-noise ratio and a high degree of fragmentation, indicated by the intense heme signal in Fig. 6a, were, however, unavoidable for IR-MALDI in this wavelength regime. The accessible mass range was limited to $\sim$20 kDa.

2.2.7. Mechanisms of energy deposition

For all of the matrices examined in this study, significant differences were found between the spectral features of the transmission spectra and the threshold fluence for at least part of the spectral range

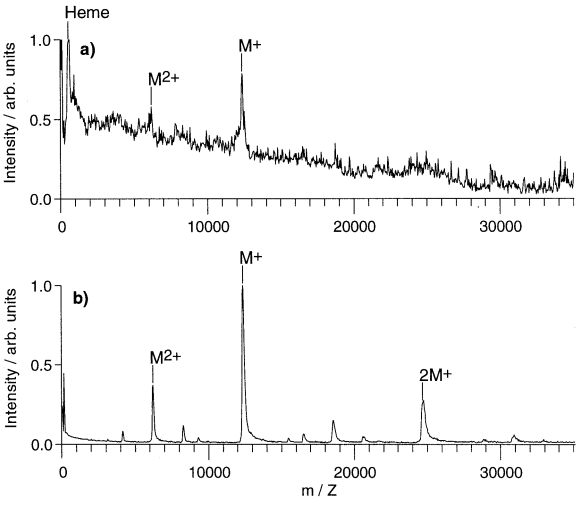

Fig. 6. IR-MALDI mass spectra of cytochrome C desorbed from a glycerol matrix with wavelengths in the overtone and fundamental region of the glycerol O–H stretch vibration: (a) LIN-TOF-IR-MALDI mass spectrum with a wavelength of $\lambda=1.45$ μm (overtone vibration), sum of 30 single-shot mass spectra; (b) REF-TOF-IR-MALDI mass spectrum with a wavelength of $\lambda=2.94$ μm (fundamental vibration), sum of 15 single-shot mass spectra.

investigated. However, at least for some matrices and limited wavelength ranges, the matrix absorption, as revealed by IR spectroscopy, seems to have a determining influence on the threshold fluence in IR-MALDI. This is particularly the case for the region of C–H stretch vibrations in alcohols, for wavelengths beyond the O–H peak absorption in carboxylic acids, and for the indole band in tryptophane. A general rejection of the principle that the threshold fluence is to first order proportional to the reciprocal of the matrix absorbance is, therefore, also not justified. The deviations from this simple model are, nevertheless, strong, particularly in the 2.7–3.3 μm wavelength region. Similar experiments and results by Cramer et al. clearly showed that these discrepancies are not caused by a contribution of the substrate absorption [17]. To explain the wavelength dependence of the threshold in this spectral range, a dominating influence of free absorbers or residual water has instead been proposed [10,12,13,15,17–19,25]. The accurate determination of the threshold fluence as a function of the wavelength for a variety of matrices, as carried out in this study, should allow an at least qualitative

assessment of the correlation between the experimental results and the two models.

A strong argument for a significant influence of free or weakly hydrogen-bound hydroxyl groups on the spectral function of the threshold fluence can be derived from a comparison of the carboxylic acid matrices that contain only carboxylic hydroxyl groups to those carboxylic acid matrices with at least one additional alcoholic or phenolic hydroxyl group. All carboxylic acids investigated show a broad wavelength plateau of low-threshold fluences and good IR-MALDI performance. This low-fluence range sets in at ~2.9 μm for matrices that contain only carboxylic hydroxyl groups (Figs. 1a,b, 3a), and at ~2.8 μm for those carboxylic acid matrices with at least one additional noncarboxylic O–H group (Figs. 1c, 3b,c). The plateau ends at the O–H absorption band of the strongly hydrogen-bound carboxylic group in the solid state (~4 μm for nicotinic acid, ~3.4 μm for all other carboxylic acids). The low wavelength onset of the plateau can be compared to the stretching vibrations of free O–H groups that are found preferentially in the gas phase or in strongly diluted solutions and polar solvents. These free hydroxyl absorptions range from 2.74 to 2.79 μm for alcohols and phenols and from 2.81 to 2.86 μm for carboxylic acids [32,33]. Here the longer wavelengths for carboxylic O–H groups can be attributed to the intramolecular hydrogen binding to the carbonyl oxygen [32]. The observed different onsets of the threshold plateaus for both groups of matrices are in agreement with the spectral difference between free carboxylic and noncarboxylic vibrations. However, the reported wavelengths of the peak absorption for the free vibrations are lower than the onset of the threshold plateaus in our measurements by up to 100 nm.

This observation can be explained if weakened rather than noninteracting hydroxyl groups are assumed to play a substantial role in the energy deposition process. The plateau in threshold fluences for carboxylic acid matrices will then correspond to a continuum of intermolecular hydrogen bond strengths, ranging from the maximum strength in the ideal crystal down to almost completely free (carboxylic or noncarboxylic) hydroxyl groups.

In case of the matrices with N–H groups as chromophores in the midinfrared, similar conclusions can be drawn. Hydrogen bonding for N–H groups is not as strong as for O–H groups. Consequently, the red shift with respect to the free vibration for the stretching vibration of hydrogen-bonded N–H groups is less pronounced (<80 nm in most cases) [32]. The expected effect on the threshold characteristic will, hence, not be as pronounced as for the O–H groups. The low thresholds at 2.90 μm for thiourea and tryptophane (Fig. 4a,b) are slightly outside the absorption band (Fig. 4c,d) but are again in good agreement with the free N–H vibration (2.86–3.03 μm) [32,33]. The smoothing of the pronounced absorption bands in the thiourea spectral threshold dependence can also tentatively be attributed to a distribution of hydrogen-bond strengths in the sample. In case of the amino acid tryptophane, a weakening of the hydrogen bond of the NH_3^+ group could, furthermore, significantly enhance the absorption in the wavelength region of relatively low threshold fluences around 3.05 μm.

For the phenolic and alcoholic matrices, a different behavior is observed. The hydrogen-bonded hydroxyl vibration bands in the transmission spectra (3.0–3.1 μm) for phloroglucinol, glycerol, and triethanolamine are blue shifted by 130–250 nm in the threshold fluence curves. The minimum threshold fluences are located around 2.87 μm for these matrices. This is still at a substantially longer wavelength than the free phenolic or alcoholic O-H peak absorptions between 2.74 and 2.79 μm. In the free absorber model, this blue shift can tentatively be assigned to a well-defined weakening of intermolecular associations in contrast to the continuum of hydrogen-bond strengths for the carboxylic acid matrices.

From a comparison of the spectral threshold dependencies of succinic acid and caffeic acid with the IR-transmission spectra of the compounds, Sheffer et al. drew very similar conclusions with respect to the role of free or weakly hydrogen-bound carboxylic and phenolic O–H vibrations as absorbers in IR-MALDI [13]. Durrant et al. also suspected a contribution of free hydroxyl groups in IR-MALDI because of the generally good performance of hydroxy substituted matrices near 2.8 μm wavelength [11]. In case of

4-nitroaniline, an assignment of free N–H absorption was judged inconclusive by Sheffer et al. because of the small wavelength shift for these functional groups on hydrogen bonding and because of the additional overlap with the water absorption [13].

The observed wavelength dependencies of the threshold fluences could, in fact, also be influenced by a contribution from the strong water absorption near 2.9 μm (residual water model). A contribution of water is supported by the fact that water was used as a solvent in all preparations. The incorporation of water in the crystal lattice, as revealed by X-ray crystallography, is however, very different for the tested matrices. Solid phloroglucinol, for example, exists as a dihydrate if crystallized from aqueous solutions [34]. The threshold dependence of phloroglucinol (Fig. 5a) between 2.80 and 3.20 μm indeed scales qualitatively quite well with the reciprocal IR absorption of water in the midinfrared [35]. Succinic acid, caffeic acid, and nicotinic acid crystals, in contrast, do not incorporate water molecules into their crystal structures [36–38]. The surprisingly low threshold fluences around 3.0 μm for these matrices could, however, possibly be induced by microinclusion of water clusters on crystallization. The inclusion of solvent clusters is a well-known artifact for organic crystals grown from solutions [39]. Klapper, for example, has reported solvent inclusions of water and methanol on a microscopic scale for thiourea [40].

The preparation of liquid matrix samples also produces a mixture of water, matrix, and analyte. Although most of the water is probably gassed off rapidly in the vacuum system at room temperature, some water may remain in the liquid sample for longer periods and contribute to the absorption around 3 μm. Finally, the hydration of the analyte molecules, if retained in the final preparation, can also be a source of residual water.

For some matrices and spectral ranges, the residual water model alone can hardly explain all experimental results. The low threshold fluence for nicotinic acid around 3.3 μm (Fig. 3a), for example, falls into a range distinctly outside the water O–H band but is, at the same time, still in the low-absorption wing of the matrix (Fig. 3d). Furthermore, if water absorption would contribute simply additively to the matrix absorption, the distinct bands of matrices like thiourea, caffeic acid, and quinic acid would not be expected to be completely masked by the contribution of the water in the threshold fluence curves.

In summary, based solely on the wavelength dependence of the threshold fluence, an influence of both weakly associated O–H and N–H groups, as well as by residual water in the 3-μm wavelength range, appears possible. Following the above argumentation, the free absorber model would, however, explain the distinct differences in the wavelength characteristics for the different chemical structures in considerably more detail.

For both mechanisms, it is not yet clear what the precise nature of the influence would be. As pointed out before, there is no evidence of a quantitative change in matrix absorption caused by the occurrence of free absorbers or residual water in typical IR-MALDI samples if these samples are investigated by IR spectroscopy [17,25]. Therefore, one has to distinguish two scenarios. In the first scenario, the actual absorption under IR-MALDI conditions is significantly different from what is measurable by standard IR spectroscopy at relatively low fluence levels. This assumption addresses a change in matrix absorption during the laser pulse via a “bootstrap” mechanism, as has been suggested previously [13,17]. In the second case, resonant energy deposition via matrix absorption, as one of the determining steps in IR-MALDI, has to be given up, at least for the spectral range around 3 μm. For these wavelengths, then, other strongly wavelength-dependent and as yet unidentified mechanisms could possibly determine the overall outcome of an IR-MALDI analysis. These mechanisms could possibly be strongly influenced by the absorption of a very few residual water molecules or chromophores with weakened hydrogen bonds. A deeper insight into the processes of energy deposition in IR-MALDI and further assessment of the proposed models is not possible based solely on the wavelength dependence of the threshold fluence. Additional experiments, presented in the second part of this article, have therefore been carried out to further elucidate whether residual water or weakened hydrogen bonds

(or both) play a dominant role in energy deposition in IR-MALDI.

4. Part II: The role of hydrogen bonds and water

4.1. Experimental

4.1.1. Laser transmission measurements

The molar decadic absorption coefficient ϵ_n under typical IR-MALDI fluence conditions was determined by focusing the laser beam through matrix samples of well-defined thickness in an external set-up in ambient air (Fig. 7a,b). In the case of succinic acid, single crystals (thickness d=100–850 μm) were used, whereas the glycerol samples consisted of thin layers

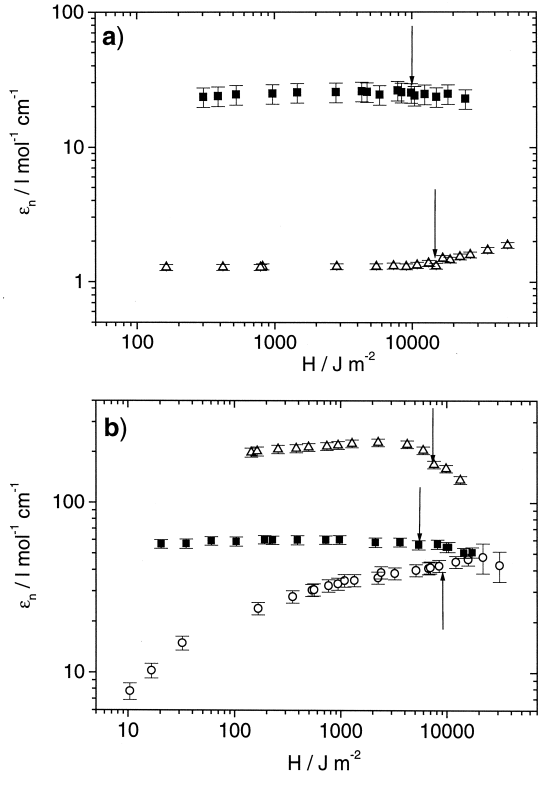

Fig. 7. Molar decadic absorption coefficient ϵ_n of succinic acid and glycerol as a function of laser fluence H and laser wavelength λ: (a) matrix, succinic acid single crystals; △ λ=2.94 μm; ■ λ=3.4 μm; (b) matrix, glycerol; ○ λ=2.79 μm; △ λ=2.98 μm; ■ λ=3.4 μm. The IR-MALDI threshold fluences for the desorption of cytochrome C ions at the different wavelengths are indicated by arrows.

(d = 10–50 μm) between cover glasses. The thickness of the sample was measured either with a standard optical microscope for the single crystals or by confocal laser scanning microscopy (CLSM) for the glycerol layers with an accuracy of approximately ±5% in both cases. To mimic IR-MALDI exposure conditions, the laser beam was focused onto the sample with a plano-convex lens of 110 mm focal length, identical to the one used for the mass spectrometric measurements. The incident laser energy E_i was measured by a high-precision energy meter (Laser Precision, Yorkville, NY). The transmitted energy E_t was monitored with a sensitive pyroelectric detector (model 420, Eltec Instruments, Daytona Beach, FL), which was calibrated against the energy meter. The experimental uncertainty in the determination of ϵ_n was calculated from the experimentally determined standard deviations in E_i, E_t, and d.

4.1.2. Temperature-controlled target stage

For some MALDI experiments, the temperature of the stainless steel sample target was varied in the range of approximately −30 and +25°C by cooling the target stage with liquid nitrogen. The target temperature was measured with a platinum resistance thermometer (PT100, Conrad Elektronik, Hirschau, Germany) as described previously [41]. Threshold fluences were determined at different temperatures during several cooling cycles.

4.1.3. Sample preparation

Unless specifically noted, solid matrix samples were prepared by the standard dried-droplet method, drying the samples in a stream of cold air over a period of several minutes. In some experiments with succinic acid, the drying step was performed rapidly within a few seconds at 10^{-2} mbar in the sample transfer chamber. These vacuum-dried preparations exhibit a more homogenous sample morphology and a higher reproducibility between different irradiation sites and from shot to shot. However, mass spectra exhibited a more pronounced cation adduct formation because of a lesser purification on crystallization. Single succinic acid crystals, some of them doped with cytochrome C, were grown over several weeks

as described previously [42]. Liquid matrix samples of glycerol were prepared on-target by thoroughly mixing the neat liquid with the aqueous analyte solution in a 1:1-volume ratio. Before insertion of the samples into the high vacuum of the sample chamber, most of the water was gassed off at a pressure of $\sim 10^{-2}$ mbar in the transfer lock of the mass spectrometer. Ice matrix preparations were made by drying a 10^{-3} M aqueous solution of cytochrome C under ambient conditions, as described previously [43]. Subsequently, these samples were frozen to liquid nitrogen temperature and rapidly transferred into the mass spectrometer. Because of the warming up of the sample stage, the time for threshold determination was limited to ~15 min.

4.2. Results and discussion

4.2.1. Influence of weakened hydrogen bonds on the threshold fluence

In the free absorber model, the unexpected wavelength dependence of the threshold around 3 μm wavelength is explained by weakly or non-hydrogen-bound O–H or N–H functional groups with a strong absorption around 2.9 μm. Such free absorbers potentially exist at the crystal surface or in the crystal lattice, for example, near analyte molecules or crystal defects [13,17–19]. A generation of free hydroxyl groups during laser irradiation has also been proposed [13,17]. As a consequence of such a bootstrap mechanism, a change in the absorption of IR-MALDI matrices under typical MALDI irradiance conditions, compared to the standard low-fluence spectroscopy, can be expected.

In this study, the possible influence of free surface absorbers on the energy deposition in IR-MALDI was assessed for three preparation techniques of succinic acid with strongly different surface-to-volume ratios. A potential influence of free, interstitial absorbers was tested by increasing the analyte-to-matrix ratio to increase the number of free boundaries in the matrix crystals. A potential change in matrix absorption during the laser exposure ("bootstrap effect") was examined for glycerol as well as for succinic acid single crystals by laser transmission measurements, covering a wide fluence range from far below to distinctly above IR-MALDI threshold fluences.

Table 1
Threshold fluences H_0 for desorption of cytochrome C ions from different preparation techniques of succinic acid in dependence of the wavelength λ

Wavelength λ/μm	Threshold fluence H_0/Jm^{-2}		
	Vacuum dried	Air dried	Single crystal
2.94	2550 ± 300	4230 ± 550	14180 ± 2510
3.40	3310 ± 380	3920 ± 530	10020 ± 1410

4.2.2. Weakened hydrogen bonds for surface molecules

To test the potential influence of surface matrix molecules with possibly different absorption characteristics than their bulk counterparts on the threshold fluences in IR-MALDI, three different succinic acid preparations, vacuum dried, air dried, and succinic acid single crystals, were compared. The very different times of crystallization for these preparations result in significantly different sample morphologies and surface-to-volume ratios. Whereas the vacuum-drying procedure generated matrix crystals of only a few micrometers in size that were homogeneously spread out over the whole sample area, the dried-droplet technique produces 150–500-μm long needles, comparable in size to the laser focus, with thicknesses ranging from 30 to 60 μm and varying in orientation. Succinic acid single crystals typically were ~0.5–3 mm in size, with thicknesses ranging from 100 to 800 μm. The experimentally determined mean threshold fluences and standard deviations for the generation of cytochrome C ions at the wavelengths of 2.94 and 3.40 μm and the three preparation techniques are listed in Table 1. The threshold fluences increase monotonically with crystal size for both wavelengths. This general shift to higher threshold fluences with decreasing surface-to-volume ratio can probably be attributed to a general decrease in cohesive energy for shorter times of crystallization, as it is observed for both test wavelengths. For the interpretation of the higher threshold fluences of the single crystals at both wavelengths it has to be kept in

mind that these crystals are birefringent and could possibly exhibit an orientation-dependent absorption for the linearly polarized laser light (dichroism). Laser transmission experiments with varying orientations of the crystals to the laser beam, however, did not reveal an influence of such an effect on the described experiments.

More interestingly, with respect to the free absorber model, different spectral courses of the threshold fluences were found for different preparation techniques. Whereas the threshold fluence is significantly lower at 2.94 than at 3.40 μm for the vacuum-dried preparations, the threshold is equal within the measurement uncertainty at both wavelengths for the dried-droplet method. In case of the succinic acid single crystals, threshold fluences were even found to be ~30% lower at 3.40 than at 2.94 μm. The latter behavior was observed, however, only for single crystals with almost perfect crystallographic planes. Single crystals with rougher surfaces caused by crystallographic defects tended to exhibit the threshold dependence of the dried-droplet preparations. The threshold fluences for the generation of matrix ions from pure succinic acid preparations showed very similar trends. This proves that the observed effects were at least not the result of an accumulation of analyte molecules near the surface.

The dissimilar wavelength dependencies for different preparation techniques can tentatively be explained if surface matrix molecules of succinic acid dominantly influence the IR-MALDI response around 3 μm wavelength. In case of the vacuum-dried preparation, absorption by an increased number of surface molecules less strongly hydrogen-bound than their bulk counterparts effectively blue-shifts the minimum threshold fluence into the 3 μm region. For the succinic acid single crystals, in contrast, the relative contribution by surface chromophores will be far less. Consequently, the wavelength dependence for the single crystals reflects, at least qualitatively, the bulk transmission spectrum at the selected wavelengths (see Fig. 1[d]).

A dominating influence of a constant fraction of surface absorbers, however, is in strong contradiction to the exponential increase in signal intensity with increasing laser fluence, determined recently for succinic acid at 2.94 μm wavelength and a uniform laser beam profile [27]. Furthermore, even for the vacuum-dried microcrystals only a few micrometers in size, the fraction of surface molecules relative to the overall number of matrix molecules in the excited sample volume is relatively small for a laser penetration depth on the order of 100 μm (see below). In fact, IR spectroscopy of thin microcrystalline succinic acid samples, produced by fast evaporation with acetone as solvent at ambient pressure, showed no qualitative change in the spectral course of absorption relative to the conventional IR transmission or absorption spectra [17,25]. In terms of the free absorber model, it must, hence, be concluded that either a minority of surface absorbers effectively influences the threshold fluence in IR-MALDI with succinic acid, while the overall matrix absorption remains unaffected, or that the very high energy deposition via surface molecules initiates a bootstrap mechanism with an increase in absorption during the laser pulse that cannot be detected by IR-spectroscopy.

In a recent publication, Papantonakis et al. also suggested a putative dominant role of surface molecules in IR-MALDI around 3 μm [19]. A strong influence of the sample morphology on the threshold fluence for two different regimes of crystal growth in air-dried succinic acid preparations was also reported by Hess et al. [18]: Smaller dentritic crystals with a greatly increased surface area generally showed a considerably lower threshold than larger crystals. Hess et al. proposed the generation of analyte ions predominantly from near-surface analyte molecules. Consequently, a similar wavelength dependence for different sample morphologies was proposed by the authors, contradictory to the results reported in Table 1. Sheffer and Murray observed a lower-threshold fluence at 3.0 than at 3.4 μm with a preparation of succinic acid on a nitrocellulose layer [13]. The use of nitrocellulose resulted in more homogeneous samples and a higher reproducibility of the ion signal. In view of the above results, the assumption of an increase in the number of surface absorbers in preparations with a nitrocellulose comatrix and a, therefore, similar wavelength dependence of the threshold fluences, as

for the vacuum-dried preparations in Table 1, appears reasonable.

4.2.3. Weakened hydrogen bonds of bulk molecules

In principle, weakly hydrogen bonded matrix molecules at matrix–analyte boundary interfaces in the crystal could also explain or enhance the observed results. It has to be kept in mind, however, that the mechanism(s) of analyte incorporation into matrix crystals are not known; in particular, the details of the interaction between the matrix and analytes. The potential influence of incorporated analyte molecules on the hydrogen bonds of the crystal lattice has been studied by determining the influence of the molar analyte-to-matrix (A/M) ratio on the threshold fluence for wavelengths of 2.9 and 3.4 μm. For both wavelengths, a comparable decrease in threshold fluence by ~30% was observed when the A/M ratio was varied from 5×10^{-6} to 5×10^{-4}.

This wavelength-independent uniform decrease in threshold with A/M ratio can probably be assigned to the physical detection limit. A minimum number of analyte ions has to reach the detector to produce a sufficient threshold signal. For more dilute samples, a larger amount of sample needs to be desorbed at a higher fluence to generate this threshold number. As no wavelength dependence of the threshold fluence on the A/M ratio is observed, it can be assumed that a generation of free absorbers at analyte/matrix interfaces is either negligible or does not significantly influence the threshold. The first assumption is supported by investigations of Cramer et al. and Durrant et al., who did not detect frequency shifts in the IR absorption spectra of IR-MALDI matrices cocrystallized with analytes [15,44].

4.2.4. Dynamic generation of weakened hydrogen bonds during the laser exposure

If weakened hydrogen bonds are generated during the laser pulse, a change in absorption as a function of laser fluence can be expected. Such a process was investigated by laser transmission measurements over a wide fluence range from significantly below to above IR-MALDI threshold fluence values. Fig. 7 shows the dependence of the molar decadic absorption coefficient ϵ_n on the incident laser fluence for succinic acid single crystals (Fig. 7a) and glycerol layers (Fig. 7b) at a few selected wavelengths.

In the case of the succinic acid single crystals (Fig. 7a), the absorption remains constant over more than two orders of magnitude in fluence for the two wavelengths of 2.94 μm (low absorption of associated O–H groups but potentially high absorption by "free" O–H groups) and 3.40 μm (peak absorption of the associated O–H groups in succinic acid). The threshold fluences for the generation of cytochrome C ions in succinic acid single-crystal preparations at the two wavelengths are indicated by arrows.

A very different behavior was found for glycerol (Fig. 7b). In this case, only the absorption coefficient for the C–H stretch vibration at 3.40 μm is independent of the laser fluence. The absorption at the 2.79 μm wavelength increases monotonically with fluence, whereas for the 2.98 μm wavelength and fluences above ca. 3500 J m^{-2}, the absorption declines as a function of fluence. At the threshold fluence for the generation of cytochrome C ions out of a glycerol matrix, indicated by the arrows in Fig. 7(b), the combined effect of the bleaching of the absorption at 2.98 μm but an ongoing increase at 2.79 μm wavelength can be interpreted as a substantial blue-shift of the O–H stretching vibration band.

Such a blue-shift is expected to occur on weakening of the intermolecular hydrogen bonds of the hydroxyl group. A similar dynamic change in the absorption of the hydroxyl group, as observed here for glycerol, has been reported for transient heating of water with lasers of different pulse durations ranging from 10 ps to some hundred nanoseconds [45,46]. The effect is attributed to a weakening of hydrogen bonds on the temperature rise in the sample during the laser exposure. The blue-shift of the O–H stretch absorption in water with increasing temperature is also accompanied by a loss of band intensity for the O–H band [45]. It is reasonable to assume that for glycerol a laser-induced transient heating weakens the intermolecular hydrogen bonds and shifts the O–H stretching mode in a presumably similar manner as for H_2O, while the C–H group remains unaffected. Qualitatively, such a blue-shift and loss of band intensity is in

good agreement with the observed spectral dependence of the threshold fluence (Fig. 5b). At least for glycerol, the discrepancies between wavelength-dependent threshold fluence and IR spectroscopy can, therefore, be explained by this effect.

One has to pay attention to the fact that the laser transmission experiments as given in Fig. 7(b) only represent the absorption coefficient averaged over the sample thickness of at least 10 μm and the entire laser-pulse width. For an accurate determination of the deposited energy per unit volume at threshold fluence in a glycerol matrix, one has to take the temporal evolution of the absorption into account. Therefore, the dynamic absorption model developed by Cummings and Walsh for laser pulses with Gaussian temporal profiles [47,48] was used to analyze the experimentally determined functional dependence of $\epsilon_n(H, \lambda)$ on fluence. Values of 1.0×10^9, 2.5×10^9, and 1.3×10^9 J m^{-3} for the absorbed energy per unit volume for a 50-nm thick surface layer result with the dynamic absorption model for the individual threshold fluences at the three wavelengths of 2.79, 2.98, and 3.40 μm, respectively. These values are identical within a factor of 2.5, whereas the low-light intensity IR-transmission curve (Fig. 5[e]) would have suggested a difference in energy per volume by at least a factor of six. The calculated deposited energy per volume is also in good agreement to values determined recently for an Er:YAG-laser at $\lambda=2.94$ μm with a flat-top beam profile and a longer pulse width of 100 ns [27] and also with previous measurements for UV-MALDI and various matrices [23,49]. The values computed by the dynamic absorption model correspond to a temperature rise in the thin glycerol layer between 350 and 800 K. The deposited energy at fluences of about ion threshold can also be compared to the enthalpy of vaporization for glycerol of 1.25×10^9 J m^{-3} (at 298 K) [50]. Although the spectral shift in absorption is presumably of thermal origin and enough energy for vaporization is principally available even at threshold, it has to be pointed out that a purely thermal desorption mechanism is rather unlikely. In particular, translational temperatures of IR-MALDI ions far beyond any reasonable thermal evaporation temperature have been demonstrated in measurements of the initial energy distributions [51].

For succinic acid, the situation is very different. The results of Fig. 7(a) clearly show that the absorption at both test wavelengths remained unaffected by the laser fluence even up to the maximum applied fluence. On the basis of the transmission measurements of a single crystal, the molar decadic extinction coefficients from Fig. 7a correspond to a laser penetration depth of 230 μm at 2.94 μm and to 12 μm at 3.40 μm wavelength, respectively. A deposited energy in the top monolayers of a succinic acid single crystal of 6×10^7 J m^{-3} at 2.94 μm and of 8×10^8 J m^{-3} at 3.4 μm is calculated at the threshold fluences for both wavelengths. This large difference in energy per volume at the two wavelengths contrasts strongly to the only relatively small range of deposited energies at the threshold with the glycerol matrix. Furthermore, at least the 2.94 μm value is far below the heat of fusion and sublimation of succinic acid, as has been pointed out before [17,27,42].

Cramer et al. [17] have discussed a solid-state disintegration in IR-MALDI via a spallation process—originally developed by Dingus and Scammon to describe low-energy solid-state rupture by acousto-mechanic strain [52]. On the basis of this model, a peak stress amplitude of 300 bar at 2.94 μm and of 2100 bar at 3.40 μm wavelength in case of the succinic acid single crystals can be calculated near threshold. For the stress amplitude at the 3.40 μm wavelength, the acousto-mechanical energy loss during the pulse duration out of the excited volume was taken into account [52]. Fissures in single crystals near the irradiated area have indeed been observed in our experiments at both wavelengths, indicating a strong mechanical stress, in agreement with the model and similar observations at $\lambda=2.94$ μm by Cramer et al. and Kampmeier et al. [17,42]. Because of the seven-times-higher stress amplitude at 3.40 μm as compared to 2.94 μm, the wavelength dependence of the threshold fluence is, however, inconsistent with a simple spallation model, although the values for the stress amplitude, given above, appear to be in principle high enough to initiate material removal by laser irradiation in IR-MALDI. The observed independence

of the absorption coefficient on fluence for bulk succinic acid in Fig 7a is not a surprise because the temperature rise in the upper matrix layer, calculated from the determined absorption coefficient ϵ_n of 1.4 l mol^{-1} cm^{-1} at 2.94 μm, is only 30 K at threshold fluence, as has also been pointed out by Talrose et al. [25]. The hydrogen bonds between the matrix dimers in carboxylic acids are easily formed and quite strong. A dimer absorption band for these groups can be found even in dilute solutions in polar solvents and in the vapor state at low temperatures [32].

However, it has to be noted that a change in absorption of only a superficial layer near the surface may not show up in the transmission experiments. In this case, the weakening of the hydrogen bonds during the laser pulse can possibly be induced either by instantaneous stress or thermal expansion of a few microns-thick surface layer. In summary, the bootstrap mechanism, suggested by Cramer et al. and Sheffer and Murray to overcome the discepancies between absorption and threshold fluence around 3-μm wavelength for succinic acid [13,17], can not be deduced from our measurements. However, its existence and impact on the energy absorption as such can also, at least for a small surface layer, not be completely ruled out.

4.2.5. Influence of residual water on the threshold fluence

In the residual water model, the surprisingly low threshold fluences around 3 μm wavelength could originate from the absorption by trapped crystal water or the water of hydration of the analyte molecules. A possible role of residual water as an absorber in IR-MALDI is supported by previous results of Berkenkamp et al. for the mass spectrometric analysis of frozen hydrated proteins ("ice" preparation) at 2.94 μm wavelength prepared without any additional organic matrix [43]. In some previous studies, the influence of the water absorption on the threshold fluence in IR-MALDI was assessed by deuterium exchange experiments using D_2O as solvent for matrix and analyte [15,17,25], as the peak absorption of water around 2.94 μm shifts to about 4.0 μm in heavy water. With D_2O as solvent and test wavelengths around 2.9 μm, lower spectra qualities [25] and an increase in threshold fluence by a factor of about two [17] were found for succinic acid as a matrix; for a 7-hydroxy-coumarin matrix, the change to heavy water even led to a loss in analyte ion generation [15]. However, all these deuterium exchange experiments suffer from the severe problem that the observed effect could also be induced by a change in the absorption of the deuterated matrix (any use of heavy water in the preparation procedure in MALDI necessarily leads to a partial or even complete deuteration of the IR-active groups of the matrix, resulting in a similar red-shift of the matrix absorption as for water).

To test the residual water model in this study, a different experimental approach was therefore followed that takes advantage of the different optical properties of water above and below 0°C. Whereas the absorption coefficient of a matrix compound like succinic acid should stay constant for a small change in temperatures around 0°C, the phase transition to ice causes a significant red-shift in the peak absorption wavelength of water [53,54]. Consequently, if absorption by water molecules is responsible for the surprisingly low threshold fluence around 3 μm, the phase transition should result in a noticeable change in the wavelength dependence of the threshold fluence. To address the possible influence of the water of hydration as a potential absorber, further experiments with a reduced protein hydration were carried out. The studies also were extended to varying water contents in liquid glycerol samples.

4.2.6. Freezeable residual water

The absorption of water in the 3-μm wavelength region is determined by the symmetric (ν_1) and asymmetric (ν_3) O–H stretch vibrations. Both bands overlap in water and are additionally in Fermi resonance with the first overtone frequency of the water bending vibration (ν_2), resulting in a relatively broad absorption band (Fig. 8a). On the basis of spectroscopic studies of HDO, Ford and Falk reported a change in the peak absorption and in the half-width of the different vibrational modes on the phase transition from water to ice [53]. The peak absorption of the ν_3

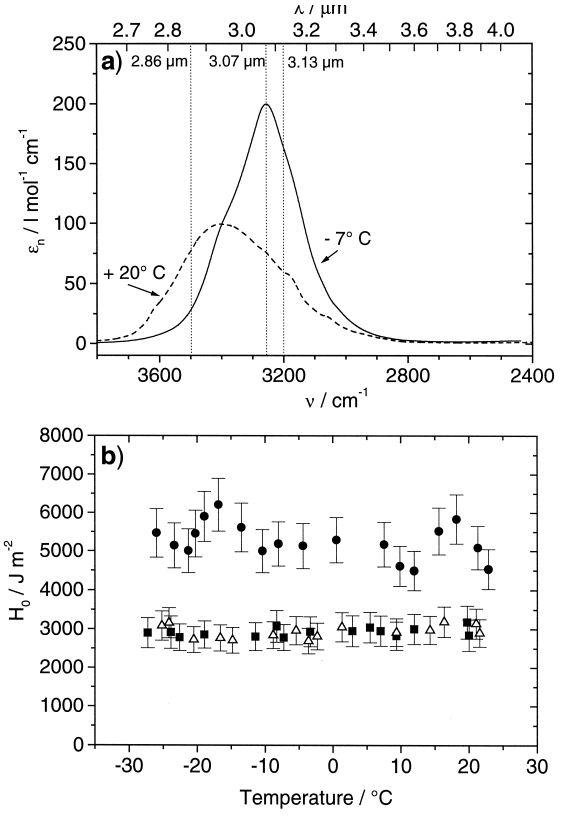

Fig. 8. (a) Molar decadic absorption coefficient ϵ_n of H_2O as a function of wavenumber ν and wavelength λ for different temperatures T: dashed line, T=25°C (liquid water); solid line, T=−7°C (ice). ϵ_n was calculated from the imaginary part of the complex refraction index tabulated in [35] and [57]. The dotted lines indicate the wavelengths used in this study for the determination of threshold fluences at different sample temperatures (see text for explanation). (b) Threshold fluence H_0 for desorption of cytochrome C ions from a succinic acid matrix at different wavelengths λ as a function of sample temperature T: ● λ=2.86 μm; △ λ=3.07 μm; ■ λ=3.13 μm.

mode, for example, was found to shift from 2.96 μm in liquid water to 3.03 μm in ice close to 0°C [53]. Simultaneously, the width $\Delta\lambda$ of the absorption band was found to sharpen from $\Delta\lambda$=220 nm to $\Delta\lambda$=55 nm. Because of the band overlap in H_2O, maximal changes in the absorption coefficient on the phase change from liquid to ice can be expected (Fig. 8a) for the test wavelengths of 2.86 μm (decrease in absorption) as well as for 3.07 and 3.13 μm (increase in absorption). If (freezeable) water plays a dominant role as an absorber in IR-MALDI, a corresponding shift in the threshold fluence as a function of the sample temperature should be measurable for these test wavelengths. Experimentally, however, no systematic shift in the threshold fluence at the H_2O phase transition was observed within the experimental uncertainty in threshold determination for any of the tested wavelengths (Fig. 8b). The results presented in Fig. 8b were obtained for the vacuum-dried preparations to achieve optimal reproducibility. Measurements with air-dried (dried-droplet) preparations and with succinic acid single crystals showed a similar behavior.

These results do not necessarily exclude any influence of water absorption in IR-MALDI, as only "free" water, like microinclusion of water in organic crystals or the outer hydration shells of biopolymers, is expected to undergo the phase transition and spectral change. Strongly hydrogen-bonded water molecules, for example, in glycerol/water mixtures, will go undetected by this method. For solvated DNA strands it has been shown by Falk et al. that only an inner layer of the hydration shell of biomolecules is incapable of freezing [53]. This "bound" water of the inner shells was found to retain the absorption properties of free liquid water despite the assumed strong hydrogen bonding to the biopolymer. Ice bands were found only if the water content exceeded ∼13 water molecules per nucleotide [53]. With respect to these results, further experiments were carried out to investigate the influence of nonfreezeable solvent water and the inner hydration layers on the threshold fluence.

4.2.7. "Residual" water in glycerol/water mixtures

To test the potential influence of the water content in the hygroscopic glycerol matrix, 200 pmol cytochrome C was dissolved in mixtures of glycerol and water, with glycerol:water volume ratios ranging from 15:1 to 1:2. Samples were frozen by dumping the target into liquid nitrogen for several minutes before insertion into the mass spectrometer. This procedure ensured a conservation of the water content under high-vacuum conditions for a sufficiently long measuring time. With the molar decadic absorption coefficients taken from Fig. 7b and Fig. 8a and the

densities of glycerol and water, one calculates a two-times-higher absorption per volume of H_2O than for glycerol at 2.94 μm. An increase in the water content should, therefore, reduce the threshold fluence if water acts as a matrix in IR-MALDI.

Experimentally, at 2.94 μm wavelength, the threshold fluence remained almost constant on increasing the water content per volume until the water content of the sample approximately exceeded that of glycerol. For higher water contents, up to two times higher threshold fluences were recorded. A general change of the cohesive energy of the sample on dilution with water can be excluded in this case because no change in threshold fluence was observed for the C–H stretch vibration of glycerol at 3.4-μm wavelength, where the water absorption is very low. Therefore, at wavelengths where water absorbs, it raises the threshold fluence instead of diminishing it, at least for glycerol preparations, in contrast to the residual water model.

A similar behavior was reported before for the performance of IR-MALDI with ice as a matrix [43]. All attempts with samples of bulk, frozen aqueous solutions gave only very unsatisfactory results. However, protein spectra could be obtained if the water content was reduced to the level of water of hydration [43]. Samples had to be frozen to retain a sufficient fraction of this water in the vacuum. At room temperature no protein signals were obtained. These experiments are often taken as an indication for the influence of the water absorption in IR-MALDI. Therefore, we have investigated the wavelength dependence of such frozen hydrated preparations that contain no additional matrix.

4.2.8. Residual water in frozen hydrated preparations

The threshold fluences for the generation of singly charged cytochrome C ions for a frozen hydrated sample in dependence of the laser wavelength are presented in Fig. 9. A minimum threshold fluence is observed at ~2.98 μm, followed by a broad range of intermediate threshold fluences between 3.1 and 3.5 μm. This minimum threshold fluence is blue-shifted by ~100 nm with respect to the ice peak absorption in

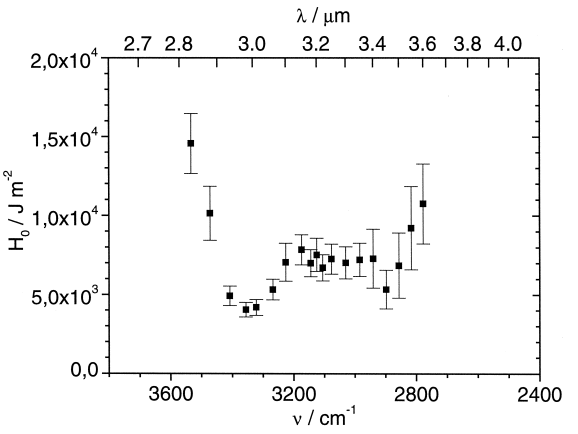

Fig. 9. Threshold fluence H_0 for desorption of cytochrome C ions from a frozen hydrated ("ice") preparation without additional matrix as a function of wavenumber ν and wavelength λ.

the applied temperature range of approximately −100°C to 0° (Fig. 8a). Surprisingly, a good IR-MALDI performance for this kind of preparation, comparable to wavelengths around 3.0 μm, and intermediate threshold fluences are found around 3.45-μm wavelength, where water (ice) is transparent. At sample temperatures >0°C, analyte ion signals disappeared at all wavelengths.

On the basis of these results, an energy deposition into the sample solely by excitation of water vibrational modes is not conceivable. Rather, the conservation of some water of hydration by freezing the sample seems necessary to facilitate desorption, for example, by an effective isolation of the analyte molecules from each other. The threshold-wavelength curve in Fig. 9, however, shows low threshold fluences at the amide A (with a peak absorption at around 3.03 μm) and less intensive amide B bands (around 3.25 μm), commonly observed in proteins [55]. The maximum absorption for cytochrome C is reported at 3.04-μm wavelength [30]. This latter value is only slightly higher than the minimum in threshold (Fig. 9). A substantial infrared absorption in the wavelength range of 3.20 to 3.50 μm caused by the NH_3^+ group of hydrated lysine residues (19% relative frequency in cytochrome C) can also be expected. Therefore, an absorption of laser light by the protein itself or by some of its amino acid residues

without any influence of residual water over the whole wavelength range with good spectra quality and low threshold fluence seems reasonable. Consequently, the observation of IR-MALDI signals from frozen hydrated samples cannot be taken as a direct proof that water (ice) is a potential absorber in the MALDI process. Berkenkamp et al. had already suspected a different role of the ice matrix compared to MALDI with organic matrices [43]. Because of the extremely low content of residual water in such frozen hydrated "ice preparations," it was suggested that a substantial fraction of the energy is deposited into the analyte itself, in agreement with the wavelength studies presented here.

These results do nevertheless not exclude that the threshold fluence, particularly for the carboxylic acids around 2.9 μm wavelength, is influenced by residual water of hydration to some extent. We have therefore extended our threshold studies further to matrix-analyte systems with a reduced level of protein hydration.

4.2.9. Reduced protein hydration

A prerequisite for a possible influence of the water of hydration on the threshold fluences is the conservation of the inner hydration shells under high-vacuum conditions at room temperature. On the basis of the observation that no analyte signal can be obtained from frozen hydrated samples >0°C, the conservation of the hydration shells in IR-MALDI at room temperature seems possible only on the incorporation of analyte molecules in the matrix crystal. To prohibit this incorporation, vacuum-dried neat succinic acid matrix layers were covered with lyophilized cytochrome C flakes. This procedure ensured a close contact of matrix and analyte molecules without incorporation of the protein into the matrix crystal. Such isolated protein clusters should loose most of their hydration shells at room temperature under high-vacuum conditions.

With this kind of preparation, no wavelength dependence of cytochrome C spectra was observed in the range between 2.9 and 3.4 μm. Assuming (a) a quantitative dehydration of analyte molecules with this preparation procedure; (b) no contribution of trapped water in the matrix, as derived above; and (c) a very low bulk absorption of succinic acid at 2.9 μm, the uniform mass spectrometric performance from 2.9 to 3.4 μm wavelength is inconsistent with the residual water model. An accurate assessment of the threshold fluence for the generation of cytochrome C ions from this kind of preparation at the different wavelengths could, however, not be made, because of an overall poor signal-to-noise ratio combined with a strong spot size dependence.

In yet another experiment, the long-term stability of the threshold fluence for succinic acid dried-droplet preparations at 2.94 μm wavelength has been followed. Even after several days under high-vacuum conditions, no significant change in threshold fluence was determined, contradictory to the residual water model, assuming that most probably, a reduction of the water content in the sample occurs by this procedure.

4.3. Conclusions

The experimental results presented in the two parts of this article provide reasonable evidence that the energy deposition in midinfrared MALDI is determined by matrix properties. IR-MALDI-sensitive vibrational modes can be either O–H, N–H, or C–H stretching vibrations of the solid or liquid state or less strongly hydrogen-bonded modes of these functional groups. The latter mechanism is presumably responsible for the strong discrepancies between the wavelength dependence of the threshold fluences and the bulk matrix absorption between 2.7 and 3.3 μm wavelength that are described in the first part of this study in agreement with prior results by other authors [11,13,15,17–19].

The possible role of weakened hydrogen bonds in IR-MALDI around 3 μm wavelength is supported by the good spectral correspondence of the wavelength-dependent threshold fluences for a variety of matrices to the expected absorption by weakly interacting O–H or N–H groups. In particular, the different threshold characteristics for matrices containing either only carboxylic or additional noncarboxylic hydroxyl groups indicate an influence of the absorption by

weakened hydroxyl groups. These assumptions are further supported by additional experiments presented in the second part of this publication. For glycerol as a matrix, a direct experimental evidence for a fluence-dependent weakening of hydrogen bonds via a dynamic bootstrap mechanism during absorption of the laser pulse energy has been demonstrated. This mechanism is most probably of thermal origin and can reasonably explain the blue-shift of the glycerol O–H band in the wavelength dependence of the threshold fluence. Taking such a dynamic absorption behavior into account, the deposited energy per volume is calculated to be rather independent of the wavelength. Its value is, furthermore, in good agreement with values for the deposited energy determined previously for UV-MALDI.

In case of succinic acid, the assessment of the predominant mechanism of energy deposition is more difficult, particularly for the region of low bulk absorption around 3 μm wavelength. A dynamic generation of weakened hydrogen bonds comparable to the glycerol results was not observed in the laser transmission experiments. However, at least a significant influence of weakly hydrogen-bound surface matrix molecules on the wavelength characteristic was found experimentally. It seems, therefore, reasonable to assume that the desorption and/or ionization around 3 μm wavelength of succinic acid is also driven by energy deposition via weakly hydrogen-bound hydroxyl groups, although the details of this mechanism remain obscure to date.

Further experiments are necessary to elucidate the actual nature of the underlying processes. In a first approach, the nature of such an energy deposition needs to be clarified in particular whether it predominantly drives the disintegration of the solid or the ionization process for succinic acid. For such experiments, the necessary separation of the desorption and ionization processes in IR-MALDI can in principle be achieved by additional postionization of the desorbed neutral molecules or by measurements of the recoil momentum of the ablated material. Preliminary measurements of the recoil momentum under IR-MALDI conditions with a piezolelectric PVDF transducer were recently presented [56].

Whether other matrix compounds, which also showed discrepancies between threshold function and IR absorbance, behave more like succinic acid or more like glycerol can hardly be predicted. A bootstrap effect, as observed for glycerol, appears likely for phloroglucinol and triethanolamine, two matrices that also show a strong blue-shift of the O–H absorption in the threshold fluence wavelength dependence. The molar decadic extinction coefficient of thiourea at 2.94 μm wavelength was recently determined to 100–200 l mol^{-1} cm^{-1} [27], quite close to the glycerol absorption value. With this absorption and a correspondingly high temperature rise, a thermal bootstrap mechanism appears likely for the relatively weak hydrogen bonds of the thiourea N–H group, in contrast to presumably all carboxylic acids with their strong intermolecular associations of the carboxylic group.

Although the wavelength-dependent threshold fluences for a variety of matrices reported in Part I might suggest an influence of residual water absorption, no further experimental evidence for such an additional absorption by free or bound residual water of crystallization or hydration was found for wavelengths at ~3 μm. In addition, the relatively good IR-MALDI performance for the frozen hydrated samples without an additional matrix for wavelengths far off the ice absorption speaks against water as the only absorber in these experiments.

Acknowledgements

This work was done in partial fulfillment of the requirements for the degree of Dr. rer. nat. of C. M. at the University of Münster. We thank T. Kues of the University of Münster for performing the CLSM measurements and V. Horneffer for her assistance with the crystallography of matrices. Financial support by grant Hi 285/8-2 of the German National Research Council (DFG) and by grant IVA1-800 985 96 of the Department of Education and Research (MWF) of the State of Nordrhein-Westfalen is greatly appreciated.

References

[1] M. Karas, F. Hillenkamp, Anal. Chem. 60 (1988) 2299.

[2] S. Berkenkamp, C. Menzel, M. Karas, F. Hillenkamp, Rapid Commun. Mass Spectrom. 11 (1997) 1399.
[3] S. Niu, W. Zhang, B.T. Chait, J. Am. Soc. Mass Spectrom. 9 (1998) 1.
[4] C. Menzel, S. Berkenkamp, F. Hillenkamp, Rapid. Commun. Mass Spectrom. 13 (1999) 26.
[5] M.M. Siegel, K. Tabei, A. Kunz, I.J. Hollander, R.P. Hamann, D.H. Bell, S. Berkenkamp, F. Hillenkamp, Anal. Chem. 69 (1997) 2716.
[6] R. Cramer, W.J. Richter, E. Stimson, A.L. Burlingame, Anal. Chem. 70 (1998) 4939.
[7] S. Berkenkamp, F. Kirpekar, F. Hillenkamp, Science 281 (1998) 260.
[8] A. Overberg, M. Karas, U. Bahr, R. Kaufmann, F. Hillenkamp, Rapid Commun. Mass Spectrom. 4 (1990) 293.
[9] A. Overberg, M. Karas, F. Hillenkamp, Rapid Commun. Mass Spectrom. 5 (1991) 128.
[10] K.L. Caldwell, D.R. McGarity, K.K. Murray, J. Mass Spectrom. 32 (1997) 1374.
[11] M. Sadeghi, Z. Olumee, X. Tang, A. Vertes, Z.X. Jiang, A.J. Henderson, H.S. Lee, C.R. Prasad, Rapid Commun. Mass Spectrom. 11 (1997) 393.
[12] C. Menzel, S. Berkenkamp, K. Dreisewerd, F. Hillenkamp, Proc. 46th ASMS Conf. Mass. Spectrom. and All. Topics, Orlando, FL, 1998, p. 922.
[13] J.D.Sheffer, K.K. Murray, Rapid Commun. Mass Spectrom. 12 (1998) 1685.
[14] W.Zhang, S. Niu, B.T. Chait, J. Am. Soc. Mass Spectrom. 9 (1998) 879.
[15] E.E. Durant, R.S. Brown, Proc. 46th ASMS Conf. Mass. Spectrom. and All. Topics, Orlando, FL, 1998, p. 929.
[16] R. Cramer, F. Hillenkamp, R.F. Haglund, J. Am. Soc. Mass Spectrom. 7 (1996) 1187.
[17] R. Cramer, R.F. Haglund, F. Hillenkamp, Int. J. Mass Spectrom. Ion Processes 169/170 (1997) 51.
[18] W. P. Hess, H.K. Park, O. Yavas, R.F. Haglund, Appl. Surf. Sci. 127–129 (1998) 235.
[19] M. Papantonakis, M. Baltz-Knorr, D. Ermer, R.F. Haglund, Proc. 47th ASMS Conf. Mass. Spectrom. and All. Topics, Dallas, TX, 1999.
[20] M. Karas, D. Bachmann, U. Bahr, F. Hillenkamp, Int. J. Mass Spectrom. Ion Processes, 78 (1987) 53.
[21] D.A. Allwood, R.W. Dreyfus, I.K. Perera, P.E. Dyer, Appl. Surf. Sc. 109/110 (1997) 154.
[22] F. Hillenkamp, M. Karas, U. Bahr, A. Ingendoh, in: A. Hedin, B.U.R. Sundquist, A. Benninghoven (Eds.), Ion Formation from Organic Solids, Wiley, Chichester, 1990, p. 111.
[23] X. Chen, J.A. Carroll, R.C. Beavis, J. Am. Soc. Mass Spectrom. 9 (1998) 885.
[24] V. Horneffer, K. Dreisewerd, H.C. Lüdemann, F. Hillenkamp, M. Läge, K. Strupat, Int. J. Mass Spectrom. Ion Processes, 185/186/187 (1999) 859.
[25] V.L. Talrose, M.D. Person, R.M. Whittal, F.C. Walls, A.L. Burlingame, M.D. Baldwin, Rapid Commun. Mass Spectrom. 13 (1999) 2191.
[26] K.L. Caldwell, K.K. Murray, Appl. Surf. Sci. 127–129 (1998) 242.
[27] D. Feldhaus, C. Menzel, S. Berkenkamp, F. Hillenkamp, K. Dreisewerd, J. Mass Spectrom. 35 (2000) 1320.
[28] D.N. Nikogosyan, Properties of Optical and Laser-Related Materials, Wiley, Chichester, 1997, p. 208.
[29] DMS Working Atlas of Infrared Spectroscopy, Butterworths, London, 1972.
[30] R.J. Keller, The Sigma Library of FT-IR spectra, Vol. 1 and 2, Sigma Chemical Company, 1986.
[31] R. Mecke, F. Langenbuecher, Infrared Spectra, Heyden, Freiburg, 1964.
[32] L.J. Bellamy, The Infrared Spectra of Complex Molecules, third ed., Chapman and Hall, London, 1975.
[33] M. Hesse, H. Meier, B. Zeeh, Spektroskopische Methoden in der organischen Chemie, Thieme, Stuttgart, 1991.
[34] S.C. Wallwork, H.M. Powell, Acta Cryst. 10 (1957) 48.
[35] V.M. Zolotarev, A.V. Demin, Opt. Spectrosc. (USSR) 43 (1977) 271.
[36] W.B. Wright, G.S.D. King, Acta Cryst. 6 (1953) 305.
[37] J.S. Broadley, D.W.J. Cruickshank, J.D. Morrison, J.M. Robertson, F.R.S. Shearer, H.M.M. Shearer, Proc. R. Soc. Ser. A 251 (1959) 441.
[38] S. Garcia-Granda, G. Beurskens, P.T. Beurskens, Acta Cryst. C43 (1987) 683.
[39] K.T. Wilke, Kristallzüchtung, Harri Deutsch, Thun, 1988.
[40] H. Klapper, J. Crystal Growth 15 (1972) 281.
[41] M. Schürenberg, K. Dreisewerd, S. Kamanabrou, F. Hillenkamp, Int. J. Mass Spectrom. Ion Processes 172 (1997) 89.
[42] J. Kampmeier, K. Dreisewerd, M Schürenberg, K. Strupat, Int. J. Mass Spectrom. Ion Processes 169/170 (1997) 31.
[43] S. Berkenkamp, M. Karas, F. Hillenkamp, Proc. Nat. Acad. Sci. 93 (1996) 7003.
[44] R. Cramer, PhD thesis, University of Muenster, Germany, (1997).
[45] K.L. Vodopyanov, J. Chem. Phys. 94 (1991) 5389.
[46] H. Graener, G. Seifert, A. Laubereau, Phys. Rev. Let. 66 (1991) 2092.
[47] J.P. Cummings, J.T. Walsh, Appl. Phys. Lett. 62 (1993) 1988.
[48] J.T. Walsh, J.P. Cummings, Lasers Surg. Med. 15 (1994) 295.
[49] K. Dreisewerd, M. Schürenberg, M. Karas, F. Hillenkamp, Int. J. Mass Spectrom. Ion Processes 141 (1995) 127.
[50] M. Bastos, S.O. Nilsson, M.D.M.C. Ribeiro Da Silva, M.A.V. Ribeiro Da Silva, I. Wadsö J. Chem. Thermodyn. 20 (1988) 1353.
[51] S. Berkenkamp, C. Menzel, F. Hillenkamp, Proc. 47th ASMS Conf. Mass. Spectrom. and All. Topics, Dallas, TX, 1999.
[52] R.S. Dingus, R.J. Scammon, SPIE Proceedings of Laser-Tissue Interaction II, International Society for Optical Engineering, Bellingham, WA, 1427 (1991) 45.
[53] T.A. Ford, M. Falk, Can. J. Chem. 46 (1968) 3579.
[54] M. Falk, A. G. Poole, C. G. Goymour, Can. J. Chem. 48 (1970) 1536.
[55] G.D. Thomas Jr., in: E.G. Brame, J.G. Grasseli (Eds.), Infrared and Raman Spectroscopy, Part C, Marcel Dekker, New York, 1977.
[56] K. Dreisewerd, C. Menzel, A. Rohlfing, F. Hillenkamp, L.M. Kukreja, Proc. 48th ASMS Conf. Mass. Spectrom. and All. Topics, Long Beach, Ca, 2000, p. 1657.
[57] S. Warren, Appl. Optics, 8 (1984) 1206.